

# Warps and Cosmic Infall

Ing-Guey Jiang and James Binney

*Theoretical Physics, University of Oxford, Oxford, OX1 3NP*

## ABSTRACT

N-body simulations show that when infall reorientates the outer parts of a galactic halo by several degrees per Gyr, a self-gravitating disk that is embedded in the halo develops an integral-sign warp that is comparable in amplitude to observed warps. Studies of angular-momentum acquisition suggest that the required rate of halo reorientation is realistic for galaxies like the Milky Way.

**Key words:** Warps: galaxies

## 1 INTRODUCTION

Galactic warps are common but remain mysterious. Bosma (1978) showed that of order one half of all galactic HI disks are measurably warped, as is the disk of the Milky Way. Briggs (1990) studied the warps of a sample of 12 galaxies in some detail and inferred several general laws that govern the phenomenology of warps.

Theoretical studies of warps have made substantially less progress, so that after four decades of work on this problem, there is no consensus as to how warps work and why they are so common. An explanation that has enjoyed some success since it was first mooted (Toomre 1983; Dekel & Shlosman 1983) is that warps persist indefinitely because they are normal modes of oscillation of the disk in the potential of a flattened massive halo. Recently it has emerged that this proposal fails completely when proper account is taken of the internal dynamics of the halo (Nelson & Tremaine 1995; Binney, Jiang & Dutta 1998 – hereafter Paper I). Consequently, there has been renewed interest in other possible explanations. Ostriker & Binney (1989) pointed out that the net angular-momentum vector of a typical galactic halo must significantly shift its direction every Hubble time or so, and that the resulting torques are liable to warp any galactic disk. In particular they investigated the possibility that such torques caused the misalignment of the Milky Way’s inner and middle disks.

Ostriker & Binney did not attempt to reproduce the Galaxy’s warp in the same way because of the undefined nature of the dynamics of the dark halo in the case that the halo is disturbed by accretion. Garcia-Ruiz, Kuijken & Dubinski (1998) briefly report a first attack on this problem, in which the halo is rotated rigidly. Here we describe experiments in which a fully dynamical halo of  $10^5$  particles reorientates its angular-momentum vector as a result of accreting fresh material. A disk comprising 100 massive rings is embedded in the halo. We show that this disk develops an integral-sign warp very similar to those actually observed.

## 2 THE COMPUTER CODE

Our computer code and model galaxy are described in detail in Paper I, so here we only summarize them and indi-

cate differences between the present simulations and those described in Paper I. The halo is represented by a standard  $N$ -body code in which the potential is found by expanding the density on a polar grid in spherical harmonics. The disk consists of massive rings that couple to each other by direct summation of the vertical forces between rings, under the assumption that the maximum excursion of any ring from the  $xy$  plane is small compared to the ring’s radius. The torques on rings from the halo are calculated from the spherical-harmonic expansion for the halo’s potential. Conversely, the rings exert forces on the halo particles because the rings contribute to the latter expansion. Thus, complete symmetry is maintained in each type of interaction (ring-ring, ring-particle and particle-particle) while ensuring that the disk is a tightly coupled entity. The sum over spherical harmonics is carried up to and including  $l = 8$  and then truncated. Paper I describes numerical checks on the accuracy of the code.

## 3 THE GALAXY MODEL

The surface density of the disk, which is represented by 100 rings, is exponential with scale-length  $R_d$  out to  $R_t = 3.5R_d$ . At  $R > R_t$  the surface density is smoothly tapered to zero at  $R_0 = 4R_d$ . At the start of the simulation the disk lies flat within the equatorial plane of the halo.

The halo is represented by  $10^5$  particles and has a total mass ten times that of the disk; consequently, the average mass of a ring is 100 times the mass of a halo particle. The particles are distributed such that the circular-speed of the combined disk and halo is very nearly flat out to  $5R_d$ . Further out the circular-speed curve gradually drops, becoming Keplerian at  $R > 14R_d$ . The halo is flattened along the symmetry axis of the disk, with initial axis ratio  $\sim 0.77$ . In one simulation the halo has no net rotation. In another the halo is caused to rotate in the same sense as the disk by reversing the angular momentum,  $L_z$ , about the disk’s spin axis of one fifth of the halo particles: this was done by picking halo particles at random and reversing  $L_z$  if this was opposite in sign to  $L_z$  for the disk.

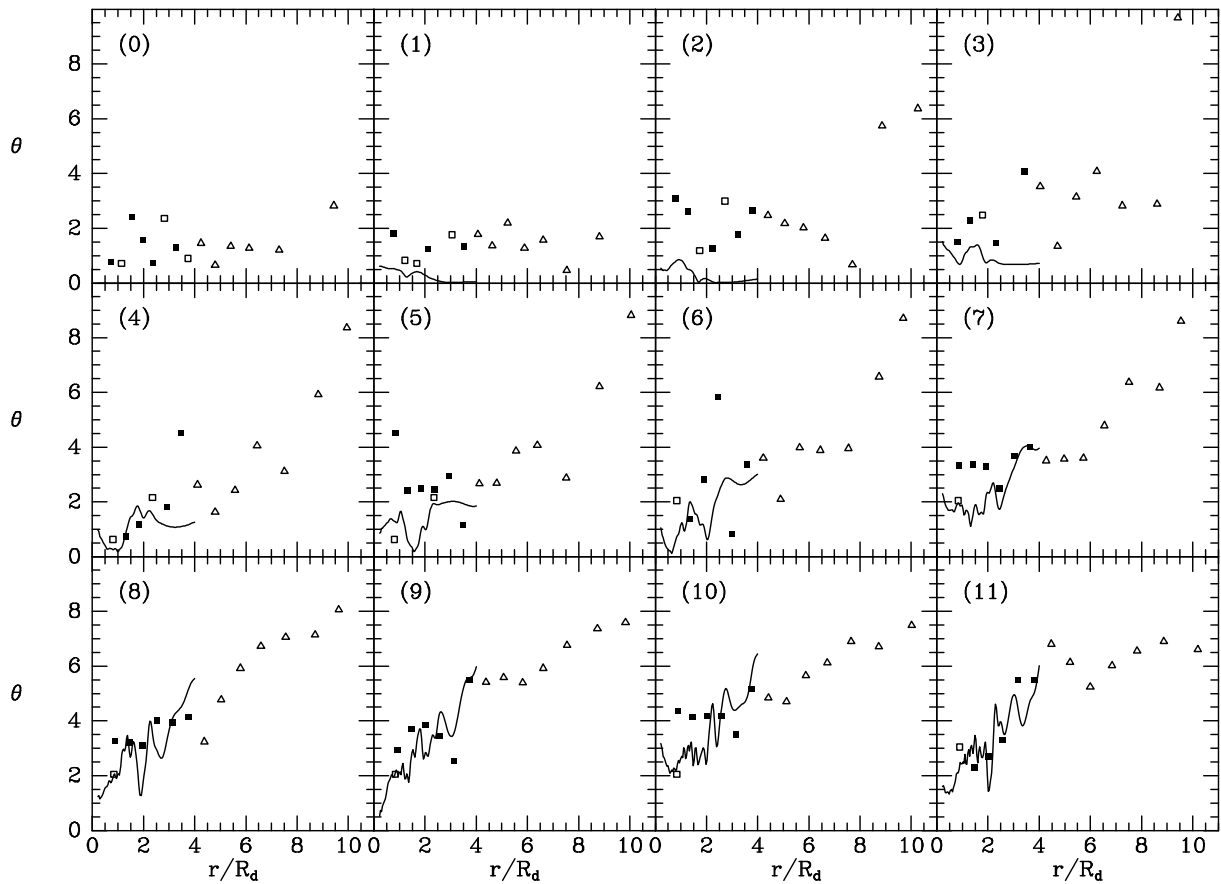


**Figure 1.** In each panel the curve shows, as a function of radius, the inclination  $\theta_d$  of the disk to its original symmetry axis while the points show the inclination of the halo to the same axis. Filled symbols indicate that the halo is inclined in the same sense as the disk, and open symbols indicate the opposite sense of inclination. Beyond the edge of the disk, the halo's inclination is marked by triangles. Between successive panels a time has elapsed which is equal to  $\sim 2.3$  times the time,  $t_{\text{ref}}$ , required to travel the halo's half-mass radius at the rms speed of a halo particle. In this simulation the halo has no net rotation.

#### 4 MODELLING INFALL

We model infall of material by steadily injecting particles in a toroidal region. Specifically, in an appropriately oriented coordinate system, each added particle has coordinates

$$\begin{aligned} x &= (a + s \cos \theta) \cos \phi \\ y &= (a + s \cos \theta) \sin \phi \\ z &= s \sin \theta, \end{aligned} \quad (1)$$

where  $a = 8.9R_d$  and  $\theta$  and  $\phi$  are angles that are uniformly distributed in  $(0, 2\pi)$ . The variable  $s$  in equation (1) is a random variable chosen such that the surface probability density is

$$P(s) = \frac{s}{b^2} e^{-s^2/2b^2} \quad (2)$$

with  $b = 0.11R_d$ . Thus, the injection torus is characterized by radii  $a$  and  $b$  with  $a/b = 80$  and has an approximately Gaussian density profile when sliced perpendicular to its larger circle. The symmetry axis of the torus is tilted by  $15^\circ$  with respect to the disk's initial spin axis, so that the torus passes above the  $x$  axis of the disk at  $x > 0$ . The initial velocities of injected particles are directed tangentially around the torus, in the sense of disk rotation, and are equal in magnitude to the local circular speed at the moment of injection.

A useful characteristic time is the time required to travel a distance equal to the halo's half-mass radius ( $\sim 3.2R_d$ ) at the rms speed of a halo particle. If we call this time  $t_{\text{ref}}$ , then a fresh batch of particles was injected each  $2.3t_{\text{ref}}$  such that the number of particles that had been injected up to time  $t$  is given by

$$N_{\text{inj}}(t) = 15000 [1 - \cos(\pi t/t_{\text{max}})], \quad (3)$$

where  $t_{\text{max}} = 25t_{\text{ref}}$  is the duration of the simulation. As equation (3) implies, in all 30000 particles, or 30% of the original halo mass, were injected.

#### 5 DIAGNOSTICS

We wish to describe the orientation of each of the disk's rings and to relate this to the shape of the halo's mass distribution at a similar radius. To this end, for each ring, we determine the angle  $\theta_i$  between the ring's axis and the original symmetry axis of the disk, as well as the azimuthal angle  $\phi_i$  of the ring's lowest point.

We determine the shape of the halo as a function of radius  $r$  from the coefficients  $A_{lm}(r)$  and  $B_{lm}(r)$  used to expand the halo's density in spherical harmonics [equation (16) of Paper I]. As is well known, for given  $l$  the complex coefficients  $X_{lm} = A_{lm} - iB_{lm}$  transform under rotations

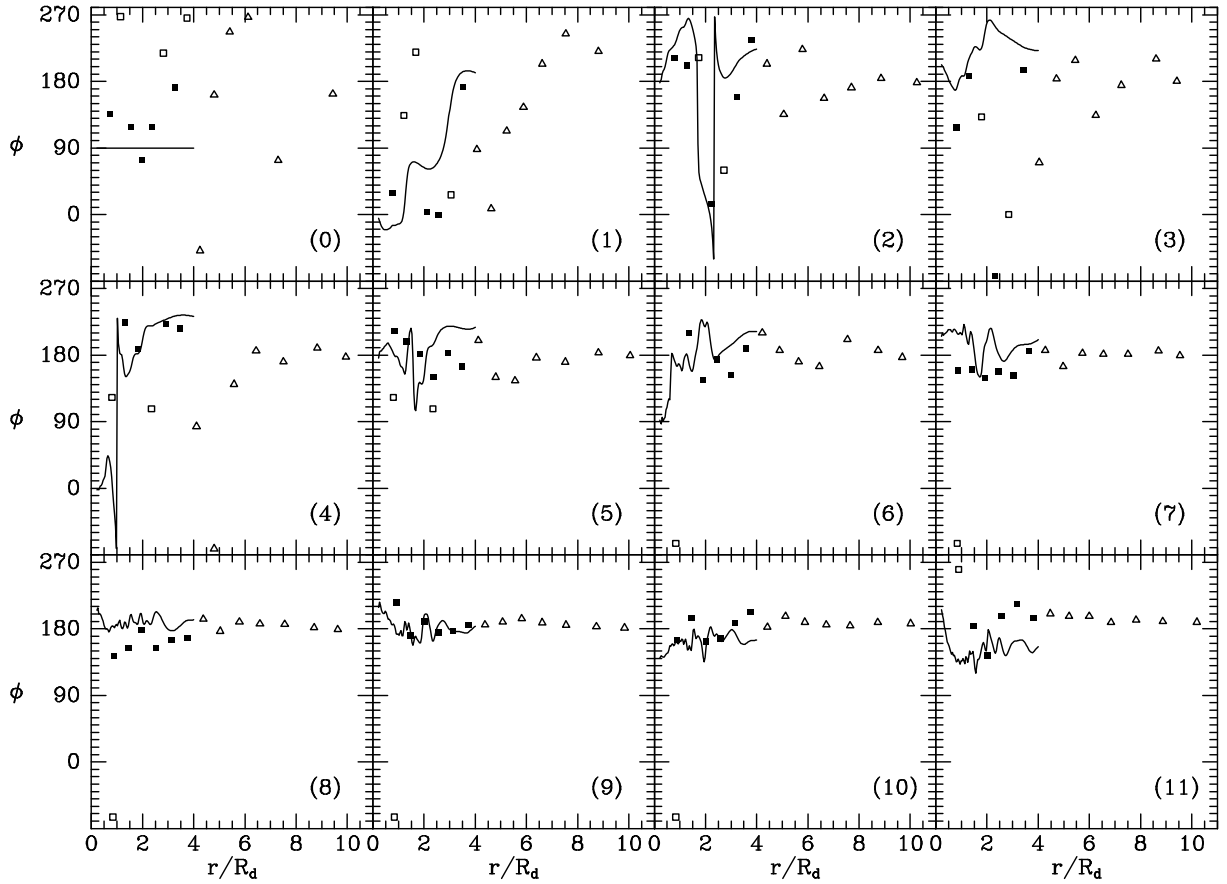


**Figure 2.** The same as Fig. 1 except that the angles marked are the values of  $\phi_d$  (curves) and  $\phi_h$  (points).

of the coordinate system that defines the polar angles, as the spin- $l$  irreducible representation of the rotation group,  $O(3)$ . Hence, once the  $X_{lm}$  have been determined in any given frame, their values  $X'_{lm}$  in any rotated frame may be obtained by multiplying by the spin- $l$  matrix for the relative orientation of the two frames. The coefficient  $X'_{20}(r)$  will be largest when the  $z$  axis of the rotated system most nearly coincides with the shortest principal axis of the halo at radius  $r$ , and we determine the direction of this axis by maximizing  $|X'_{20}|^2$  with respect to the Euler angles  $\theta$  and  $\phi$  upon which it depends. Since this procedure does not distinguish between a direction and its opposite, it does not distinguish between  $(\theta, \phi)$  and  $(\theta', \phi') = (\pi - \theta, \phi + \pi)$ . We resolve this ambiguity by requiring  $\theta$  to be smaller than  $\pi/2$ .

## 6 RESULTS

Figs 1 and 2 compare, as functions of  $r$ , the polar angles  $\theta_d$  and  $\phi_d$  that specify the direction of each ring's symmetry axis (curves) with the angles  $\theta_h$  and  $\phi_h$  that specify the direction of the shortest principal axis of the halo (points). For ease of interpretation, the halo's angles are plotted as full points when  $|\phi_d - \phi_h| < 90^\circ$ , and as open points otherwise. Hence, full points indicate that the halo and disk are tilted in similar directions, while open points indicate that the two components are tilted in opposing directions.

In the top left panel of Fig. 1, which describes the initial condition, the disk's curve is invisible because it runs along

the  $x$ -axis and the halo points give an idea of the statistical error in the determination of  $\theta_h$ . In the second panel the disk can be seen to have developed a small corrugation. The equal numbers of open and filled squares that describe the halo in this panel indicate that the disk and the halo are not systematically aligned at this time, probably because the disk's small corrugation merely reflects statistical noise in the simulation. By the panel labeled 3, the outer halo has clearly developed a systematic tilt of order  $3^\circ$ . By the time of panel 5, the preponderance of filled halo points in the region of the disk suggests that the halo's tilt has been to some extent communicated to the disk. In the next few panels it becomes steadily clearer that the tilt is propagating from the outer halo inwards, and causing the inner halo and disk to tilt very much as a unit. By the time of panel 9 both  $\theta_h$  and  $\theta_d$  increase essentially linearly with radius from  $\sim 2^\circ$  at  $r \lesssim R_d$  to  $\sim 5.5^\circ$  at  $r \sim 4R_d$ . The increase of  $\theta_d$  with  $R$  implies that the disk has developed an integral-sign warp, with the outermost ring moving  $\sim 0.3R_d$  out of the plane of the innermost ring. For the case of the Milky Way, for which  $R_d \simeq 3$  kpc, this would correspond to a warp amplitude of order 1 kpc at 14 kpc, very similar to that actually measured (Burton 1992).

Fig. 2 compares the azimuth of the ascending node of the disk,  $\phi_d$ , with the corresponding azimuth,  $\phi_h$  for each spherical shell of the halo. Initially,  $\phi_d$  is arbitrarily set to  $90^\circ$  and statistical fluctuations cause  $\phi_h$  to be widely scattered. By the time of panel 5, the scatter in  $\phi_h$  has

been reduced to  $\sim 40^\circ$ , and this scatter continues to decrease as further infall causes the halo to become more and more inclined to the  $z$ -axis of the coordinate system. The disk is closely aligned with the halo from panel 5 on. The mean value of  $\phi_d$  shows a statistically marginal tendency to decrease from the times of panel 8 to that of panel 11, consistent with the disk precessing retrogradely in the gravitational field of the outer halo. It is not clear, however, that this precession, if statistically significant, is other than a transient phenomenon.

The results for the case of a slowly rotating halo are essentially identical to those for the non-rotating case that are shown in Figs 1 and 2.

## 7 CONCLUSIONS

We have shown that a realistic warp develops in a disk embedded in a live halo when the halo accretes material whose angular-momentum vector is inclined slightly with respect to the original symmetry axis of the galaxy. Is this mechanism the long-sought solution to the warping problem?

The close alignment of the disk with the local halo that is evident in both the simulations presented here and in Paper I indicates that a warp is essentially a *halo* phenomenon: the disk serves largely as a handy tracer of the halo's dynamics. The essential feature of our halo simulation is the realignment of the approximate symmetry axis of the halo at  $r \simeq 10R_d$  by  $\sim 7^\circ$  over the duration,  $t_{\max}$ , of the simulation. If we scale the simulations to parameters characteristic of the Milky Way ( $R_d \simeq 3$  kpc,  $v_c \simeq 220$  km s $^{-1}$ ), we find  $t_{\max} \simeq 0.9$  Gyr. Hence, we would seem to have a convincing explanation of warp if the symmetry axis of the outer halo can shift by  $\sim 7^\circ$  in  $\sim 0.9$  Gyr.

Several authors have studied how tidal interactions endow protogalactic regions with angular momentum at early times (e.g. Heavens & Peacock 1988) and these studies are generally in good agreement with numerical simulations (Barnes & Efstathiou 1987). Ryden (1988) and Quinn & Binney (1992) investigated the rate at which the direction of infalling angular momentum should slew by studying the angular momenta of individual spherical shells of protogalactic material. Quinn & Binney found that the angular momenta acquired by shells that differ in radius by a factor 2 have a clear tendency to be antiparallel. Moreover, the angular momentum per unit mass of a shell rises strongly with radius, with the consequence that the net angular momentum of a galaxy tends to be aligned with the angular momentum of the most recently accreted shell. These two results together imply that the net spin axis of a halo tends to slew through more than  $90^\circ$  in the time required for the radius of the currently accreting shell to double. This time depends on the cosmology and the initial density profile (e.g. Fillmore & Goldreich 1984). For critical cosmic density,  $\Omega = 1$ , it is typically comparable to the current Hubble time and the halo's spin axis is likely to slew by  $\gtrsim 7^\circ$  in 0.9 Gyr.

A growing body of evidence suggests that  $\Omega$  is significantly less than unity, and one might be concerned that infall has largely dried up. In reality, it is not the global value of  $\Omega$  that is relevant here, but the effective value within the Local Group. Dynamical studies of the local group of ever greater sophistication all conclude that the mass of the Local Group is  $4 - 8 \times 10^{12} M_\odot$  (e.g., Schmoldt & Saha 1998).

If the halos of M31 and the Milky Way have flat rotation curves with amplitude  $v_c$ , their masses interior to radius  $r$  are given by

$$\frac{M}{10^{12} M_\odot} = 1.1 \left( \frac{v_c}{220 \text{ km s}^{-1}} \right)^2 \left( \frac{r}{100 \text{ kpc}} \right). \quad (4)$$

Consequently, the measured mass of the Local Group can be accommodated in the halos of these two dominant galaxies only if they touch each other. In this case, given that M31 is approaching us, parts of M31's halo would now be falling into ours, and vice versa. Thus, even if all the mass of the Local Group had in the past been somehow organized into two quiescent halos, there would still be dynamically important infall at the present epoch. In reality, there is plenty of observational evidence that the Galactic halo is profoundly affected by infall even at  $r = 20 - 60$  kpc: the Galaxy is currently accreting both the Magellanic Clouds (e.g., Murai & Fujimoto 1980) and the Sagittarius dwarf galaxy (Ibata et al. 1997). Since observations of dwarf galaxies imply that both of these systems must be tracers of much more massive streams of dark matter, the natural conclusion to draw is that most of the mass of the Local Group still lies outside the virialized halos of M31 and the Galaxy, and is falling in at a dynamically significant rate.

This being so, it seems that warps probably are caused by infall-driven reorientation of the outer parts of virialized halos.

## REFERENCES

- Barnes J., Efstathiou G., 1987, ApJ, 319, 575
- Binney J.J., Jiang I.-G., Dutta S.N., 1998, MNRAS, 000, 000 (Paper I)
- Bosma A., 1978, PhD thesis Groningen University, the Netherlands
- Briggs F., 1990, ApJ, 352, 15
- Burton W.B., 1992, in 'The Galactic Interstellar Medium', SAAS-Fee Advanced Course 21, eds. Pfenniger, D., Bartholdi, P. Berlin, Springer
- Dekel A., Shlosman I., 1983, in IAU Symposium 100, 'Internal Kinematics and Dynamics of Galaxies', ed. E. Athanassoula, Dordrecht, Reidel, p. 187
- Fillmore J.A., Goldreich P., 1984, ApJ, 281, 1
- García-Ruiz I., Kuijken K., Dubinski J., 1998, in ASP Conf. Ser. 136, 'Galactic Halos', ed. D. Zaritsky, ASP, San Francisco
- Heavens A., Peacock J., 1988, MNRAS, 232, 339
- Ibata R., Wyse R., Gilmore G., Irwin M., Suntzeff N., 1997, AJ, 113, 634
- Murai T., Fujimoto M., 1980, PASJ 32 581
- Nelson R.W., Tremaine S., 1995, MNRAS, 275, 897
- Ostriker E.C., Binney J.J., 1989, MNRAS, 237, 785
- Quinn T.R., Binney J.J., 1992, MNRAS, 255, 729
- Ryden B.S., 1988, ApJ, 329, 589
- Schmoldt I.M., Saha P., 1998, AJ, 00, 00
- Toomre, A., 1983, in IAU Symp. 100, 'Internal Kinematics and Dynamics of Galaxies', ed. E. Athanassoula, Reidel, Dordrecht, p. 177

This paper has been produced using the Blackwell Scientific Publications  $\text{\TeX}$  macros.